



AIAA 2004-4061

**Acoustic Instability of the Slab  
Rocket Motor**

S. R. Fischbach, J. Majdalani and G. A. Flandro  
Advanced Theoretical Research Center  
University of Tennessee Space Institute

**Propulsion Conference and Exhibit**

11–14 July 2004  
Fort Lauderdale, FL

## Acoustic Instability of the Slab Rocket Motor

Sean R. Fischbach,\* Joseph Majdalani,† and Gary A. Flandro‡  
 University of Tennessee Space Institute, Tullahoma, TN 37388

This article provides rigorous mathematical details leading to an improved formulation of acoustic instability in solid rocket motors. The evaluation of stability growth rate factors is carried out both numerically and asymptotically. Analytical expressions for the stability factors are obtained over a broad spectrum of operating parameters. For all representative rocket motors under investigation, the analytical estimates exhibit an error of 5% or less. Both numerics and asymptotics converge in predicting markedly less stable systems than projected by classic stability theory. The dramatic differences can be ascribed to the dismissal of time-dependent rotational coupling in the previous formulation. The current study unravels the details of six additional growth rate corrections not accounted for previously. These include the rotational flow, mean vorticity, viscosity, pseudo acoustic, pseudo vorticity and unsteady nozzle growth rate factors. The fourth and fifth terms are due to acoustical and vortical interactions with the often neglected pseudopressure. The sixth is due to the energy associated with the unsteady rotational flow exiting the nozzle. This study enables us to isolate the impact of various flow attributes on stability. These involve the motor aspect ratio, surface Mach number, viscous parameter, oscillation mode shape number, and surface admittance. Based on the slab motor geometry, we find that the flow turning correction is cancelled identically by another rotational term not accounted for previously. We also find that the unsteady nozzle damping effect is offset by another source of instability due to the pseudopressure.

### Nomenclature

$A_p$	= unsteady pressure amplitude
$A_b^{(r)}$	= burning surface admittance
$A_S^{(r)}$	= inert surface admittance
$A_N^{(r)}$	= nozzle entrance plane admittance
$a_0$	= mean speed of sound
$e$	= unsteady energy density
$E$	= time-averaged unsteady system energy
$E_m^2$	= energy normalization function for mode $m$
$e_x, e_y$	= unit vectors in $x$ and $y$ directions
$k_m$	= wave number for axial mode $m$ , $m\pi H / L$
$L, H$	= enclosure length and half-height, $l = L / H$
$m$	= oscillation mode shape number
$M_b$	= surface Mach number, $V_b / a_0$
$\mathbf{n}$	= outward pointing unit normal vector
$p_0$	= mean pressure
$S$	= Strouhal Number, $k_m / M_b$

$\mathbf{u}$	= total velocity vector
$U_y, U_z$	= mean flow velocities normalized by $V_b$
$W$	= chamber width, $w = W / H$
$y$	= normal distance from the wall
$z, t$	= axial, and temporal coordinates
$\alpha$	= growth rate (dimensionless)
$\delta$	= viscous number, $[\nu / (a_0 H)]^{1/2}$
$\varepsilon$	= wave amplitude, $A_p / (\gamma p_0)$
$\phi(y)$	= function defined in Eq. (44)
$\gamma$	= ratio of specific heats
$\gamma_b$	= $2\gamma - (A_b + 1)$
$\nu$	= kinematic viscosity, $\mu / \rho$
$\rho$	= density
$\omega, \Omega$	= unsteady and mean vorticity magnitudes
$\psi(y)$	= exponential argument defined in Eq. (43)

### Subscripts

$b$	= refers to the simulated burning surface
$i, r$	= irrotational or rotational
$m$	= for a given mode number
$N, S$	= nozzle or inert surface

### Superscripts

*	= dimensional quantity
$\sim, \wedge$	= rotational or acoustical part
$r, i$	= part of a complex variable

\*Graduate student and Research Associate, Department of Mechanical, Aerospace and Biomedical Engineering. Member AIAA.

†Jack D. Whitfield Professor of High Speed Flows, Department of Mechanical, Aerospace and Biomedical Engineering. Member AIAA.

‡Boling Chair Professor of Excellence in Propulsion, Department of Mechanical, Aerospace and Biomedical Engineering. Associate Fellow AIAA.

## I. Introduction

THE rising popularity of the slab rocket motor among propulsion analysts may be attributed to the simple geometry that it offers. Clearly, the use of a rectangular-port motor facilitates the design of an experimental setup by incorporating flat segments, screens and window panels that can drastically improve test calibration and flow visualization capabilities. For the theoretical investigator, it permits the use of Cartesian coordinates which reduce the complexity of modeled equations and, therefore, facilitate the process of uncovering/achieving the desired solution.

The use of the (opposed plane) slab configuration in combustion stability related studies may be traced back to the work of Brownlee and Marble<sup>1-3</sup> who employed blocks of propellants in some of their laboratory experiments. More recent investigations that adopt the slab geometry include those by Casalis *et al.*,<sup>4-7</sup> Liou *et al.*,<sup>8-10</sup> Yang *et al.*,<sup>11-13</sup> Van Moorhem *et al.*,<sup>14-18</sup> Wasistho *et al.* at the Center for Simulation of Advanced Rockets (CSAR),<sup>19</sup> and Vuillot *et al.* at the Office National d'Études et de Recherches Aérospatiales (ONERA).<sup>20-26</sup> In that vein, it may be worth mentioning that scientists at both CSAR and ONERA have often utilized the planar/slab configuration as the preferred geometry to either validate their full-scale three-dimensional codes or to concentrate on one particular aspect of motor gas dynamics.

Despite the preponderance of slab-related studies, no fundamental formulation has yet been advanced to assess the acoustic instability characteristics associated with this particular geometry. Past studies have mainly focused on the circular-port configuration as evidenced by the pioneering work of Culick<sup>27-35</sup> and Flandro.<sup>36-41</sup> For this reason, it is the purpose of this paper to present the stability correction factors that arise in the two-dimensional motor chamber. This will be accomplished by evaluating the linear stability formulation introduced by Flandro and Majdalani<sup>37</sup> for the slab configuration.

## II. Geometric Model

The same nomenclature and flow descriptors adopted by Flandro and Majdalani<sup>37</sup> will be used except that a Cartesian coordinate system will be the system of choice here. The chamber will be modeled as a porous rectangular channel with internal half height/thickness  $H$ , width  $W$  and overall length  $L$ . Assuming that  $W \geq 6 \times H$ , the passive wall influence can be safely ignored,<sup>42</sup> and the problem can be treated as a case of two dimensional flow. The flux of gases due to combustion will be modeled by imposing uniform fluid injection along the walls at a constant velocity  $V_b$ . Whereas one end of the chamber is closed, the other is

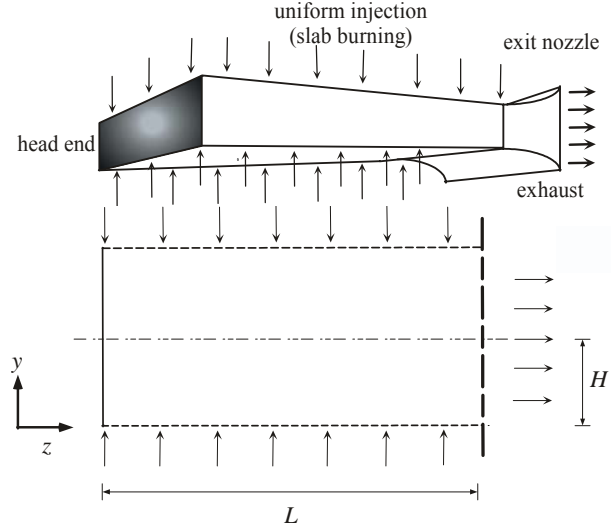


**Fig. 1** Sketches showing the physical and geometric models employed in Cartesian coordinates.

open and attached to a choked nozzle. The fluid motion in the tube is assumed to be axisymmetric and laminar. Figure 1 provides sketches of the physical as well as the geometric model.

## III. Growth Rate Calculations

Following the steps delineated by Flandro and Majdalani,<sup>37</sup> the system growth rate for a given oscillation mode can be constructed from the linear superposition of several volume integrals. Using

$$\alpha_m = \alpha_1 + \alpha_2 + \alpha_3 + \dots = \sum_{i=1}^N \alpha_i \quad (1)$$

these integrals can be carried out individually, or in combination, depending on their general form. Naturally, the composite growth rate of the system will be a linear sum of these factors. As before, a negative growth rate factor represents an energy sink, while a positive term denotes an instability contributor.

### A. First Factor: Extended Pressure Coupling

The first irrotational integrals in Ref. 37 are combined to formulate the first correction factor:

$$\alpha_1 = E_m^{-2} e^{-2\alpha_m t} \iiint_V \left\langle -\nabla \cdot \left[ \hat{p} \hat{u} + \frac{1}{2} M_b U (\hat{p})^2 \right] - M_b [\hat{u} \cdot \nabla (U \cdot \hat{u})] \right\rangle dV \quad (2)$$

Using Gauss's theorem, one transforms the integrand with the divergence operator into a simpler surface integral. One gets

$$\alpha_1 = E_m^{-2} e^{-2\alpha_m t} \underbrace{\iiint_V \left\langle -\nabla \cdot \left[ \hat{p} \hat{\mathbf{u}} + \frac{1}{2} M_b \mathbf{U} (\hat{p})^2 \right] \right\rangle}_{\text{I}} + E_m^{-2} e^{-2\alpha_m t} \underbrace{\iiint_V \left\langle -M_b [\hat{\mathbf{u}} \cdot \nabla (\mathbf{U} \cdot \hat{\mathbf{u}})] \right\rangle}_{\text{II}} dV \quad (3)$$

At this point, vector projections must be carefully evaluated along different sections of the control surfaces delineating the idealized slab motor chamber. These include, firstly, along the burning surface,

$$\mathbf{n} \cdot \hat{\mathbf{u}} = -M_b A_b^{(r)} \hat{p}, \quad \mathbf{n} \cdot \mathbf{U} = -1 \quad (4)$$

secondly, along the inert surface,

$$\mathbf{n} \cdot \hat{\mathbf{u}} = -M_b A_s^{(r)} \hat{p}, \quad \mathbf{n} \cdot \mathbf{U} = 0 \quad (5)$$

and, thirdly along the nozzle entrance plane,

$$\mathbf{n} \cdot \hat{\mathbf{u}} = M_b A_N^{(r)} \hat{p}, \quad \mathbf{n} \cdot \mathbf{U} = U_N \quad (6)$$

where  $U_N$  is the mean axial velocity crossing the nozzle entrance plane at  $z = l$ .

Knowing that  $A_s^{(r)}$  is small compared to other terms, Eqs. (4)–(6) can be substituted back into Eq. (3). The first integral becomes

$$\text{I} = -E_m^{-2} e^{-2\alpha_m t} \iint_S \left\langle -M_b A_b^{(r)} \hat{p}^2 + M_b A_N^{(r)} \hat{p}^2 + \frac{1}{2} M_b \hat{p}^2 (-1 + U_N) \right\rangle dS \quad (7)$$

Grouping and rearranging, Eq. (7) simplifies into

$$\text{I} = -E_m^{-2} e^{-2\alpha_m t} M_b \iint_S \left\langle \hat{p}^2 \left[ -A_b^{(r)} - \frac{1}{2} \right] + \hat{p}^2 \left[ A_N^{(r)} + \frac{1}{2} U_N \right] \right\rangle dS \quad (8)$$

At this juncture, one may want to insert the value of  $\hat{p}^2$  and carry out the time-averaging; this operation leads to

$$\text{I} = \frac{1}{2} E_m^{-2} M_b \left( \iint_{S_b} \left\{ \cos^2(k_m z) \left[ A_b^{(r)} + \frac{1}{2} \right] \right\} dS - \iint_{S_N} \left\{ \cos^2(k_m z) \left[ A_N^{(r)} + \frac{1}{2} U_N \right] \right\} dS \right) \quad (9)$$

In much the same way, the second integral of Eq. (3) can be written as

$$\text{II} = -E_m^{-2} e^{-2\alpha_m t} \iiint_V \left\langle M_b [\hat{\mathbf{u}} \cdot \nabla (\mathbf{U} \cdot \hat{\mathbf{u}})] \right\rangle dV = E_m^{-2} M_b e^{-2\alpha_m t} \iiint_V \left\langle (\mathbf{U} \cdot \hat{\mathbf{u}}) \nabla \cdot \hat{\mathbf{u}} \right\rangle dV \quad (10)$$

where the divergence of the mean flow vector has been set equal to zero. The latter can be expanded into

$$\text{II} = E_m^{-2} k_m M_b \iiint_V \left\langle \mathbf{U} \cdot (-\nabla \hat{p}_m / k_m) \hat{p}_m \sin^2(k_m t) \right\rangle dV \quad (11)$$

which can be written as

$$\text{II} = -E_m^{-2} M_b \iiint_V \left\langle \nabla \cdot (\mathbf{U} \hat{p}_m^2 / 2) \sin^2(k_m t) \right\rangle dV \quad (12)$$

The time-average can now be readily evaluated. One gets

$$\text{II} = -\frac{1}{2} E_m^{-2} M_b \iiint_V \nabla \cdot (\mathbf{U} \hat{p}_m^2 / 2) dV \quad (13)$$

Using Gauss's theorem, the volumetric integral can be transformed into a surface integral; one obtains

$$\text{II} = -\frac{1}{2} M_b E_m^{-2} \iint_S \left( \frac{1}{2} \mathbf{n} \cdot \mathbf{U} \hat{p}_m^2 \right) dS = \frac{1}{2} M_b E_m^{-2} \left( \iint_{S_b} \frac{1}{2} \hat{p}_m^2 dS - \iint_{S_N} \frac{1}{2} U_N \hat{p}_m^2 dS \right) \quad (14)$$

Combining Eqs. (14) and (9), Eq. (2) becomes

$$\alpha_1 = \frac{1}{2} M_b E_m^{-2} \left\{ \iint_{S_b} \frac{1}{2} \cos^2(k_m z) dS - \iint_{S_N} \left[ \frac{1}{2} U_N \cos^2(k_m z) \right] dS + \frac{1}{2} M_b E_m^{-2} \left( \iint_{S_b} \left\{ \cos^2(k_m z) \left[ A_b^{(r)} + \frac{1}{2} \right] \right\} dS + \iint_{S_N} \left\{ \cos^2(k_m z) \left[ -A_N^{(r)} - \frac{1}{2} U_N \right] \right\} dS \right) \right\} \quad (15)$$

Collecting same type integrals, one finds, at length,

$$\alpha_1 = \frac{1}{2} M_b E_m^{-2} \iint_{S_b} \cos^2(k_m z) \left[ A_b^{(r)} + 1 \right] dS - \frac{1}{2} M_b E_m^{-2} \iint_{S_N} \cos^2(k_m z) \left[ A_N^{(r)} + U_N \right] dS \quad (16)$$

which gives

$$\alpha_1 = \frac{1}{2} M_b E_m^{-2} \left\{ 2 \int_0^w \int_0^l \cos^2(k_m z) \left[ A_b^{(r)} + 1 \right] dz dx - 2 \int_0^1 \int_0^w \cos^2(k_m z) \left[ A_N^{(r)} + U_N \right] dx dy \right\} \quad (17)$$

By applying a mass balance to an internal burning slab rocket motor, one gets  $2WLV_b = 2WHU_N^*$  or  $U_N = l$ . Then using  $A_N^{(r)} = (\gamma - 1)l$ , and Eq. (17), the first growth rate factor becomes

$$\alpha_1 = \frac{1}{2} l w M_b E_m^{-2} \left[ \left( A_b^{(r)} + 1 \right) - 2\gamma \right] = \frac{4}{9} M_b \left[ \left( A_b^{(r)} + 1 \right) - 2\gamma \right] \quad (18)$$

## B. Second Factor: Dilatational Energy Correction

The fourth irrotational term leads to

$$\alpha_2 = E_m^{-2} e^{-2\alpha_m t} \iiint_V \left\langle \frac{4}{3} \delta^2 \hat{\mathbf{u}} \cdot \nabla (\nabla \cdot \hat{\mathbf{u}}) \right\rangle dV \quad (19)$$

Using the definition of acoustic velocity and pressure, one can put

$$\begin{aligned} \nabla \cdot \hat{\mathbf{u}} &= \exp(\alpha_m t) \sin(k_m t) \nabla \cdot (-\nabla \hat{p}_m / k_m) \\ &= k_m \exp(\alpha_m t) \sin(k_m t) \cos(k_m z) \end{aligned} \quad (20)$$

and so

$$\begin{aligned} \nabla (\nabla \cdot \hat{\mathbf{u}}) &= \nabla [k_m \exp(\alpha_m t) \sin(k_m t) \cos(k_m z)] \\ &= -k_m^2 \exp(\alpha_m t) \sin(k_m t) \sin(k_m z) \mathbf{e}_z \end{aligned} \quad (21)$$

turning  $\alpha_2$  into

$$\alpha_2 = -\frac{4}{3} k_m^2 \delta^2 E_m^{-2} \iiint_V \langle \sin^2(k_m z) \sin^2(k_m t) \rangle dV \quad (22)$$

After time-averaging, Eq. (19) reduces to

$$\alpha_2 = -\frac{2}{3} k_m^2 \delta^2 E_m^{-2} \iiint_V \sin^2(k_m z) dV \quad (23)$$

Using  $dV = dz dy dx$ , the triple integral can be expressed as

$$\begin{aligned} \alpha_2 &= -\frac{4}{3} k_m^2 \delta^2 E_m^{-2} \int_0^w \int_0^l \int_0^l \sin^2(k_m z) dz dy dx \\ &= -\frac{2}{3} w l k_m^2 \delta^2 E_m^{-2} [1 - \sin(2k_m l) / (2k_m l)] \\ &= -\frac{2}{3} w l k_m^2 \delta^2 E_m^{-2} = -\frac{16}{27} \xi M_b^3 \end{aligned} \quad (24)$$

## C. Third Factor: Acoustic Mean Flow Correction

The fifth term can be evaluated from

$$\alpha_3 = E_m^{-2} e^{-2\alpha_m t} \iiint_V \langle M_b \{ \hat{\mathbf{u}} \cdot (\hat{\mathbf{u}} \times \boldsymbol{\Omega}) \} \rangle dV \quad (25)$$

Being the mean flow vorticity,  $\boldsymbol{\Omega}$  can be approximated from

$$\boldsymbol{\Omega} = \Omega \hat{\mathbf{e}}_x = \frac{1}{4} \pi^2 z \cos(\theta) \mathbf{e}_x \quad (26)$$

and so

$$\hat{\mathbf{u}} \times \boldsymbol{\Omega} = \Omega \hat{u}_z \mathbf{e}_y - \Omega \hat{u}_y \mathbf{e}_z \quad (27)$$

Thus

$$\begin{aligned} \hat{\mathbf{u}} \cdot (\hat{\mathbf{u}} \times \boldsymbol{\Omega}) &= (\hat{u}_y \hat{\mathbf{e}}_y + \hat{u}_z \hat{\mathbf{e}}_z) \cdot (-\Omega \hat{u}_z \hat{\mathbf{e}}_y + \Omega \hat{u}_y \hat{\mathbf{e}}_z) \\ &= -\hat{u}_y \Omega \hat{u}_z + \hat{u}_z \Omega \hat{u}_y = 0 \end{aligned} \quad (28)$$

Evidently, substituting this result into Eq. (25) will cause  $\alpha_3$  to vanish.

## D. Fourth Factor: Flow Turning Correction

The sixth term is a function of the unsteady vorticity. Following the nomenclature introduced by Flandro,<sup>43</sup> this term will be dubbed ‘the flow turning

correction’ in the standard stability formulation based on an irrotational description of the time-dependent field. Starting with

$$\begin{aligned} \alpha_4 &= E_m^{-2} e^{-2\alpha_m t} \iiint_V \langle M_b \hat{\mathbf{u}} \cdot (\mathbf{U} \times \boldsymbol{\omega}) \rangle dV \\ &= -E_m^{-2} k_m^{-1} M_b e^{-2\alpha_m t} \iiint_V \langle \nabla \hat{p} \tan(k_m t) \cdot (\mathbf{U} \times \boldsymbol{\omega}) \rangle dV \end{aligned} \quad (29)$$

one recalls that  $\partial \tilde{u}_y / \partial z = O(M_b^2)$  so that  $\boldsymbol{\omega} = \nabla \times \tilde{\mathbf{u}} = (\partial \tilde{u}_z / \partial y) \mathbf{e}_x$ . Using the definition of  $\tilde{u}_z$ , the unsteady vorticity is expressible by

$$\boldsymbol{\omega} = \exp(\alpha_m t) \left[ \frac{\partial \tilde{u}_m^r}{\partial y} \cos(k_m t) + \frac{\partial \tilde{u}_m^i}{\partial y} \sin(k_m t) \right] \mathbf{e}_x \quad (30)$$

Using the fact that  $\mathbf{U} \times \boldsymbol{\omega} = (U_z \omega) \mathbf{e}_y - (U_y \omega) \mathbf{e}_z$ , one can rewrite  $\alpha_4$  as

$$\begin{aligned} \alpha_4 &= E_m^{-2} M_b e^{-2\alpha_m t} \iiint_V \langle [\sin(k_m z) \exp(\alpha_m t) \sin(k_m t)] \mathbf{e}_z \\ &\quad \cdot (U_z \omega \mathbf{e}_y - U_y \omega \mathbf{e}_z) \rangle dV \end{aligned} \quad (31)$$

and hence,

$$\begin{aligned} \alpha_4 &= -E_m^{-2} M_b e^{-2\alpha_m t} \iiint_V \langle \sin(k_m z) \exp(\alpha_m t) \\ &\quad \times \sin(k_m t) U_y \omega \rangle dV \end{aligned} \quad (32)$$

or

$$\begin{aligned} \alpha_4 &= -E_m^{-2} M_b e^{-2\alpha_m t} \iiint_V \langle U_y \sin(k_m z) \exp(2\alpha_m t) \sin(k_m t) \\ &\quad \times \left[ \frac{\partial \tilde{u}_m^r}{\partial y} \cos(k_m t) + \frac{\partial \tilde{u}_m^i}{\partial y} \sin(k_m t) \right] \rangle dV \end{aligned} \quad (33)$$

Equation (33) can be partitioned now into two terms

$$\begin{aligned} \alpha_4 &= \frac{-M_b E_m^{-2}}{2e^{2\alpha_m t}} \iiint_V \underbrace{\langle U_y \sin(k_m z) e^{2\alpha_m t} \sin(2k_m t) \frac{\partial \tilde{u}_m^r}{\partial y} \rangle}_{\text{I}} \\ &\quad + 2U_y \underbrace{\langle \sin(k_m z) e^{2\alpha_m t} \sin^2(k_m t) \frac{\partial \tilde{u}_m^i}{\partial y} \rangle}_{\text{II}} dV \end{aligned} \quad (34)$$

Forthwith, term I gives

$$\begin{aligned} \text{I} &= \left\langle \frac{1}{2} U_y \sin(k_m z) \exp(2\alpha_m t) \sin(2k_m t) \frac{\partial \tilde{u}_m^r}{\partial y} \right\rangle \\ &= \frac{k_m}{4\pi} \exp(2\alpha_m t) U_y \sin(k_m z) \frac{\partial \tilde{u}_m^r}{\partial y} \int_0^{2\pi/k_m} \sin(2k_m t) dt = 0 \end{aligned} \quad (35)$$

Term II can be calculated from

$$\begin{aligned}
\Pi &= \left\langle U_y \sin(k_m z) \exp(2\alpha_m t) \sin^2(k_m t) \frac{\partial \tilde{u}_m^i}{\partial y} \right\rangle \\
&= \frac{1}{2} \pi^{-1} k_m \exp(2\alpha_m t) U_y \\
&\quad \times \sin(k_m z) \frac{\partial \tilde{u}_m^i}{\partial y} \int_0^{2\pi/k_m} \sin^2(k_m t) dt \\
&= \frac{1}{2} \exp(2\alpha_m t) U_y \sin(k_m z) \frac{\partial \tilde{u}_m^i}{\partial y} \quad (36)
\end{aligned}$$

After combining its separate parts, Eq. (33) reduces to

$$\alpha_4 = -\frac{1}{2} M_b E_m^{-2} \iiint_V U_y \sin(k_m z) \frac{\partial \tilde{u}_m^i}{\partial y} dV \quad (37)$$

where the derivative must be evaluated from

$$\frac{\partial \tilde{u}_m^i}{\partial y} = -\cos \eta \exp \phi \frac{\partial (\cos \psi)}{\partial y} \sin(k_m z \cos \eta) + \dots \quad (38)$$

Only the leading term in this derivative is shown, being one order of magnitude larger than other quantities precipitated from chain-rule differentiation. The latter can be written as

$$\frac{\partial \tilde{u}_m^i}{\partial y} \approx \frac{k_m}{M_b U_y} \cos(\eta) \exp(\phi) \sin(\psi) \sin[\cos(\eta) k_m z] \quad (39)$$

Inserting Eq. (39) into Eq. (37) gives

$$\begin{aligned}
\alpha_4 &= -k_m E_m^{-2} \int_0^w dx \int_0^l \int_0^1 \cos(\eta) \exp(\phi) \\
&\quad \times \sin(\psi) \sin(k_m z \cos \eta) \sin(k_m z) dy dz \quad (40)
\end{aligned}$$

and so

$$\begin{aligned}
\alpha_4 &= -w k_m E_m^{-2} \int_0^1 \int_0^l \cos\left(\frac{1}{2} \pi y\right) \sin(k_m z) \\
&\quad \times \sin\left[\cos\left(\frac{1}{2} \pi y\right) k_m z\right] \sin(\psi) \exp(\phi) dz dy \quad (41)
\end{aligned}$$

The first integral with respect to  $z$  renders

$$\begin{aligned}
\alpha_4 &= -w k_m E_m^{-2} \int_0^1 \cos\left(\frac{1}{2} \pi y\right) \\
&\quad \times \left\{ -\frac{\sec^2\left(\frac{1}{4} \pi y\right) \sin\left[2k_m l \cos^2\left(\frac{1}{4} \pi y\right)\right]}{4k_m} \right. \\
&\quad \left. + \frac{\csc^2\left(\frac{1}{4} \pi y\right) \sin\left[2k_m l \sin^2\left(\frac{1}{4} \pi y\right)\right]}{4k_m} \right\} \\
&\quad \times \sin(\psi) \exp(\phi) dy \quad (42)
\end{aligned}$$

At this juncture, one must carefully examine the spatial behavior of each term in Eq. (42). One finds that linearization of certain terms will be appropriate prior to integration. To start, both  $\psi$  and  $\phi$  must be fully expanded using MacLaurin series; one finds

$$\psi = (k_m / M_b) \left( y + \frac{1}{24} \pi^2 y^3 + \frac{1}{384} \pi^4 y^5 + \frac{1}{322560} \pi^6 y^7 + \dots \right) \quad (43)$$

$$\phi = -\xi \left( y + \frac{1}{8} \pi^2 y^3 + \frac{11}{640} \pi^4 y^5 + \frac{241}{107520} \pi^6 y^7 + \dots \right) \quad (44)$$

It can be easily shown that the leading-order representations for  $\psi$  and  $\phi$  lead to reasonably accurate approximations. Interestingly, these simple one-term approximations perform fairly adequately. At the outset, one can put

$$\sin(\psi) = \sin(k_m y / M_b) + O(y^3) \quad (45)$$

$$\exp(\phi) = \exp(-\xi y) + O(y^3) \quad (46)$$

To be consistent, all (but the last two terms) remaining in Eq. (42) must be linearized to the order of  $y^2$ . The resulting expression for  $\alpha_4$  becomes

$$\begin{aligned}
\alpha_4 &= -w k_m E_m^{-2} \int_0^1 \sin(k_m y / M_b) \exp(-\xi y) \\
&\quad \times \left[ \frac{1}{2} l - \frac{1}{4} \sin(2k_m l) / k_m \right] dy \quad (47)
\end{aligned}$$

At first glance, the exact integral of Eq. (47) appears to be intractable. Nonetheless, an inviscid result can be extracted by suppressing the viscous parameter  $\xi$ . The inviscid form of  $\alpha_4$  turns out to be

$$\alpha_4^0 = -\frac{1}{2} w l M_b E_m^{-2} [1 - \sin(2k_m l) / (2k_m l)] \quad (48)$$

Knowing that the exact integral must match the inviscid solution in the limit as  $\xi \rightarrow 0$ , we use inductance and re-evaluate Eq. (47); at the outset, we find

$$\begin{aligned}
\alpha_4 &= -\frac{1}{2} w l M_b E_m^{-2} [1 - \sin(2k_m l) / (2k_m l)] \\
&\quad \left( 1 + M_b^2 \xi^2 / k_m^2 \right)^{-1} = -\frac{1}{2} w l M_b E_m^{-2} \times \left( 1 + M_b^2 \xi^2 / k_m^2 \right)^{-1} \\
&\quad = -\frac{4}{9} M_b \left( 1 + \pi^{-2} M_b^2 \xi^2 l^2 m^{-2} \right)^{-1} \quad (49)
\end{aligned}$$

This expression approximates Eq. (29) to within a few percent over a wide range of  $M_b$ ,  $\xi$ ,  $l$ , and  $m$ .

## E. Fifth Factor: Rotational Flow Correction

Traditionally only the integrals considered thus far have been accepted in stability assessments. Nevertheless, consistent retention of unsteady rotational terms gives rise to several additional integrals that must not be dismissed. The first rotational flow correction presented by Flandro and Majdalani<sup>37</sup> can be written as

$$\alpha_5 = e^{-2\alpha_m t} E_m^{-2} \iiint_V \langle -\tilde{\mathbf{u}} \cdot \nabla \hat{\mathbf{p}} \rangle dV \quad (50)$$

The integrand stems from

$$\begin{aligned}
-\tilde{\mathbf{u}} \cdot \nabla \hat{\mathbf{p}} &= k_m \sin(k_m z) \exp(2\alpha_m t) \\
&\quad \times \left[ \tilde{u}_m^r \cos^2(k_m t) + \tilde{u}_m^i \sin(k_m t) \cos(k_m t) \right] \quad (51)
\end{aligned}$$

so that  $\alpha_5$  can be evaluated from

$$\alpha_5 = k_m E_m^{-2} e^{-2\alpha_m t} \iiint_V \exp(2\alpha_m t) \left\langle \left[ \sin(k_m z) \tilde{u}_m^r \right. \right. \\ \left. \left. \times \cos^2(k_m t) + \sin(k_m z) \tilde{u}_m^i \sin(k_m t) \cos(k_m t) \right] \right\rangle dV \quad (52)$$

Carrying out the time-average of the last expression, one gets

$$\alpha_5 = \frac{1}{2} E_m^{-2} k_m \iiint_V \cos(\eta) \exp(\phi) \sin(\psi) \\ \times \sin[k_m z \cos(\eta)] \sin(k_m z) dV \quad (53)$$

At this point, the volume integral can be expanded into

$$\alpha_5 = k_m E_m^{-2} \int_0^w dx \int_0^l \int_0^1 \cos(\eta) \exp(\phi) \sin(\psi) \\ \times \sin[k_m z \cos(\eta)] \sin(k_m z) dz dy \quad (54)$$

This expression is the negative of Eq. (40). Following the same lines as before,  $\alpha_5$  becomes

$$\alpha_5 = \frac{4}{9} M_b \left( 1 + \pi^{-2} M_b^2 \xi^2 l^2 m^{-2} \right)^{-1} \quad (55)$$

Except for having an opposite sign, this expression is identical to the flow turning integral ( $\alpha_5 = -\alpha_4$ ). It demonstrates that, for the slab motor configuration, the flow-turning term is ‘exactly cancelled’ by the rotational flow correction both at leading order and when higher order approximations are retained. This result corresponds to the case for which the simulated burning surface extends over the entire chamber length.

## F. Sixth Factor: Mean Vorticity Correction

The fifth rotational term can be written as

$$\alpha_6 = E_m^{-2} e^{-2\alpha_m t} \iiint_V \langle M_b \tilde{\mathbf{u}} \cdot (\mathbf{U} \times \boldsymbol{\omega}) \rangle dV \quad (56)$$

This can be further simplified into

$$\alpha_6 = M_b E_m^{-2} e^{-2\alpha_m t} \iiint_V \left\langle \exp(\alpha_m t) \left[ \tilde{u}_m^r \cos(k_m t) \right. \right. \\ \left. \left. + \tilde{u}_m^i \sin(k_m t) \right] \mathbf{e}_z \cdot \left[ U_z \boldsymbol{\omega} \mathbf{e}_y - U_y \boldsymbol{\omega} \mathbf{e}_z \right] \right\rangle dV \quad (57)$$

Direct expansion gives

$$\alpha_6 = \frac{-M_b E_m^{-2}}{e^{2\alpha_m t}} \iiint_V \left\langle e^{2\alpha_m t} \left[ \left( \frac{\partial \tilde{u}_m^r}{\partial y} \right) \cos(k_m t) + \left( \frac{\partial \tilde{u}_m^i}{\partial y} \right) \right. \right. \\ \left. \left. \times \sin(k_m t) \right] U_y \left[ \tilde{u}_m^r \cos(k_m t) + \tilde{u}_m^i \sin(k_m t) \right] \right\rangle dV \quad (58)$$

After carrying out the time-averaging operation, one is left with

$$\alpha_6 = -\frac{1}{2} M_b E_m^{-2} \iiint_V U_y \left( \frac{\partial \tilde{u}_m^r}{\partial y} u_m^r + \frac{\partial \tilde{u}_m^i}{\partial y} u_m^i \right) dV \quad (59)$$

and so

$$\alpha_6 = -\frac{1}{4} M_b E_m^{-2} \iiint_V U_y \left[ \frac{\partial}{\partial y} (\tilde{u}_m^r + \tilde{u}_m^i) \right] dV \quad (60)$$

By substituting the values of  $\tilde{u}_m^r$  and  $\tilde{u}_m^i$  into Eq. (59), one collects

$$\alpha_6 = -\frac{1}{4} M_b E_m^{-2} \iiint_V U_y \cos^2(\eta) \exp(2\phi) \sin^2[k_m z \cos(\eta)] \\ \times \left\{ \sin^2(\psi) + \cos^2(\psi) \right\}_y dV \quad (61)$$

where the subscript denotes partial differentiation with respect to  $y$ . By making use of  $\sin^2(\psi) + \cos^2(\psi) = 1$ , Eq. (61) collapses into

$$\alpha_6 = -\frac{1}{4} M_b E_m^{-2} \iiint_V U_y \left\{ \cos^2(\eta) \exp(2\phi) \right. \\ \left. \times \sin^2[k_m z \cos(\eta)] \right\}_y dV \quad (62)$$

Then, by evaluating

$$\alpha_6 = -\frac{1}{4} M_b E_m^{-2} \iiint_V \left\{ \left( U_y \cos^2(\eta) \exp(2\phi) \right. \right. \\ \left. \left. \times \sin^2[k_m z \cos(\eta)] \right\}_y - \sin^2[k_m z \cos(\eta)] \right. \\ \left. \times \cos^2(\eta) e^{2\phi} \frac{\partial}{\partial y} U_y \right\} dV \quad (63)$$

the corresponding triple integral becomes

$$\alpha_6 = -\frac{1}{4} M_b E_m^{-2} \iiint_V \left\{ \left( U_y \cos^2(\eta) \exp(2\phi) \right. \right. \\ \left. \left. \times \sin^2[k_m z \cos(\eta)] \right\}_y + \frac{1}{2} \pi \sin^2[k_m z \cos(\eta)] \right. \\ \left. \times \cos^2(\eta) \sin(\eta) e^{2\phi} \right\} dV \quad (64)$$

or

$$\alpha_6 = -\frac{1}{2} w M_b E_m^{-2} \int_0^l \int_0^1 \cos^2(\eta) \exp(2\phi) \left\{ \left( U_y \right. \right. \\ \left. \left. \times \sin^2[k_m z \cos(\eta)] \right\}_y + \frac{1}{2} \pi \sin^2[k_m z \cos(\eta)] \right. \\ \left. \times \sin(\eta) \right\} dy dz \quad (65)$$

This further leads to

$$\alpha_6 = \frac{1}{2} w M_b E_m^{-2} \int_0^l \sin^2(k_m z) dz - \frac{1}{4} w \pi M_b E_m^{-2} \\ \times \int_0^l \int_0^1 \sin^2[k_m z \cos(\eta)] \cos^2(\eta) \sin(\eta) e^{2\phi} dy dz \quad (66)$$

The first integration gives

$$\alpha_6 = \frac{1}{4} E_m^{-2} M_b w \left( l - \pi \int_0^1 \cos^2(\eta) \sin(\eta) e^{2\phi} \right. \\ \left. \times \frac{1}{2} \left\{ l - \frac{1}{2} k_m^{-1} \sec\left(\frac{1}{2} \pi y\right) \sin\left[2k_m l \cos\left(\frac{1}{2} \pi y\right)\right] \right\} dy \right) \quad (67)$$

By asymptotically expanding the latter expression, one arrives at

$$\alpha_6 = \frac{1}{4} E_m^{-2} M_b w \left[ l - \pi \int_0^1 e^{2\phi} \left( \frac{1}{4} l \pi y - \frac{1}{24} l \pi^3 y^3 + \frac{1}{480} l \pi^5 y^5 + \dots \right) dy \right] \quad (68)$$

Using symbolic programming, assisted by asymptotic patching, one is able to estimate the value of the last integral from

$$\alpha_6 = \frac{1}{4} E_m^{-2} M_b w \left\{ l - \frac{1}{24} \left[ (k_m \pi \xi^4 e^{2\xi}) (\pi^2 - 12) \right]^{-1} \times \left[ \frac{39}{85} + \frac{1}{82} \xi + \frac{7}{13} \exp\left(\frac{-107}{50} \xi\right) \right] (4\pi l k_m + 3) (12\xi^2 \times (1 + 2\xi - e^{2\xi}) + \pi^2 \{ 3e^{2\xi} - 3 - 2\xi [3 + \xi(3 + 2\xi)] \}) \right\} \quad (69)$$

This expression reduces to

$$\alpha_6 = \frac{2}{9} M_b \left\{ 1 - \frac{1}{24} \left[ m\pi^2 \xi^4 e^{2\xi} (\pi^2 - 12) \right]^{-1} \times \left[ \frac{39}{85} + \frac{1}{82} \xi + \frac{7}{13} \exp\left(\frac{-107}{50} \xi\right) \right] (4m\pi^2 + 3) (12\xi^2 \times (1 + 2\xi - e^{2\xi}) + \pi^2 \{ 3e^{2\xi} - 3 - 2\xi [3 + \xi(3 + 2\xi)] \}) \right\} \quad (70)$$

### G. Seventh Factor: Viscosity Correction

The seventh and eighth rotational groups involve viscous damping expressions. In the classical stability calculations, viscous effects are discounted. A correction to the dilatational effect is represented in the seventh rotational term. Following the same procedure used before, this term can be transformed into a surface integral, viz.

$$\frac{4}{3} \iiint_V \langle \delta^2 \tilde{\mathbf{u}} \cdot \nabla (\nabla \cdot \tilde{\mathbf{u}}) \rangle dV = -\frac{4}{3} \delta^2 \iint_S \langle \mathbf{n} \cdot \tilde{\mathbf{u}} \partial p^{(1)} / \partial t \rangle dS \quad (71)$$

Clearly, Eq. (71) must be negligible insofar as it scales with the product of  $\delta^2$  (a viscous length) and the radial unsteady velocity at the boundaries.

The eighth term with viscous damping is not quite negligible. Starting with

$$\alpha_7 = E_m^{-2} e^{-2\alpha_m t} \iiint_V \langle -\delta^2 (\hat{\mathbf{u}} + \tilde{\mathbf{u}}) \cdot (\nabla \times \boldsymbol{\omega}) \rangle dV \quad (72)$$

one may set

$$\alpha_7 = \delta^2 E_m^{-2} \exp(-2\alpha_m t) \iiint_V \langle A + B \rangle dV \quad (73)$$

where  $A = -\hat{\mathbf{u}} \cdot (\nabla \times \boldsymbol{\omega})$  and  $B = -\tilde{\mathbf{u}} \cdot (\nabla \times \boldsymbol{\omega})$  so that

$$A = -\hat{\mathbf{u}} \cdot (\nabla \times \boldsymbol{\omega}) = e^{\alpha_m t} \sin(k_m z) \sin(k_m t) \frac{\partial^2 \tilde{\mathbf{u}}}{\partial y^2} \quad (74)$$

$$B = -\tilde{\mathbf{u}} \cdot (\nabla \times \boldsymbol{\omega}) = e^{\alpha_m t} \left[ \tilde{u}_m^r \cos(k_m t) + \tilde{u}_m^i \sin(k_m t) \right] \frac{\partial^2 \tilde{\mathbf{u}}}{\partial y^2} \quad (75)$$

Using standard descriptors, the second derivative can be partitioned into

$$\frac{\partial^2 \tilde{\mathbf{u}}}{\partial y^2} = \exp(\alpha_m t) \left[ \frac{\partial^2 \tilde{u}_m^r}{\partial y^2} \cos(k_m t) + \frac{\partial^2 \tilde{u}_m^i}{\partial y^2} \sin(k_m t) \right] \quad (76)$$

Substituting back into  $A$  and  $B$ , one gathers

$$A = \sin(k_m z) \exp(2\alpha_m t) \times \left[ \frac{\partial^2 \tilde{u}_m^r}{\partial y^2} \sin(k_m t) \cos(k_m t) + \frac{\partial^2 \tilde{u}_m^i}{\partial y^2} \sin^2(k_m t) \right] \quad (77)$$

and

$$B = \exp(2\alpha_m t) \left[ \tilde{u}_m^r \frac{\partial^2 \tilde{u}_m^r}{\partial y^2} \cos^2(k_m t) + \tilde{u}_m^i \frac{\partial^2 \tilde{u}_m^i}{\partial y^2} \sin^2(k_m t) + \tilde{u}_m^r \frac{\partial^2 \tilde{u}_m^i}{\partial y^2} \cos(k_m t) \sin(k_m t) + \tilde{u}_m^i \frac{\partial^2 \tilde{u}_m^r}{\partial y^2} \cos(k_m t) \sin(k_m t) \right] \quad (78)$$

When substituted back into Eq. (73), time-averaging enables us to reduce these expressions into

$$\alpha_7 = \frac{1}{2} \frac{\delta^2}{E_m^2} \iiint_V \left[ \tilde{u}_m^r \frac{\partial^2 \tilde{u}_m^r}{\partial y^2} + \tilde{u}_m^i \frac{\partial^2 \tilde{u}_m^i}{\partial y^2} + \sin(k_m z) \frac{\partial^2 \tilde{u}_m^i}{\partial y^2} \right] dV \quad (79)$$

Using the same asymptotic rationale for expanding Eq. (39), one can put

$$\frac{\partial^2 \tilde{u}_m^i}{\partial y^2} \approx \left( \frac{k_m}{M_b U_y} \right)^2 \cos(\eta) \exp(\phi) \cos(\psi) \sin[\cos(\eta) k_m z] \quad (80)$$

and

$$\frac{\partial^2 \tilde{u}_m^r}{\partial y^2} \approx -\left( \frac{k_m}{M_b U_y} \right)^2 \cos(\eta) \exp(\phi) \sin(\psi) \sin[\cos(\eta) k_m z] \quad (81)$$

The integral becomes

$$\alpha_7 = \frac{1}{2} E_m^{-2} \delta^2 k_m^2 M_b^{-2} \iiint_V \left\{ \sec(\eta) \exp(\phi) \cos(\psi) \sin(k_m z) \times \sin[k_m z \cos(\eta)] - \exp(2\phi) \sin^2[k_m z \cos(\eta)] \right\} dV \quad (82)$$



Asymptotically, it can be shown that

$$\begin{aligned} & \left| \sec(\eta) \exp(\phi) \cos(\psi) \sin(k_m z) \sin[k_m z \cos(\eta)] \right| \\ & \ll \left| \exp(2\phi) \sin^2[k_m z \cos(\eta)] \right| \end{aligned} \quad (83)$$

Therefore, this integral collapses into

$$\alpha_7 = -\frac{1}{2} E_m^{-2} \delta^2 k_m^2 M_b^{-2} \iiint_V \exp(2\phi) \sin^2[k_m z \cos(\eta)] dV \quad (84)$$

As usual, expanding the triple integral renders

$$\begin{aligned} \alpha_7 = & -E_m^{-2} \delta^2 k_m^2 M_b^{-2} \int_0^w \int_0^l \int_0^1 \{ \exp(2\phi) \\ & \times \sin^2[k_m z \cos(\eta)] \} dy dz dx \end{aligned} \quad (85)$$

so that

$$\begin{aligned} \alpha_7 = & -\frac{1}{2} w E_m^{-2} \delta^2 k_m^2 M_b^{-2} \int_0^1 \exp(2\phi) \left\{ l - \frac{1}{2} k_m^{-1} \right. \\ & \left. \times \sec(\eta) \sin[2k_m l \cos(\eta)] \right\} dy \end{aligned} \quad (86)$$

Recalling Eq. (44), subsequent linearization and integration lead to

$$\begin{aligned} \alpha_7 = & -\frac{1}{8} (24lk_m - \pi^3)^{-1} w E_m^{-2} \delta^2 \xi^{-3} k_m M_b^{-2} \\ & \times \left[ \frac{21}{32} + \frac{19}{56} \exp\left(-\frac{27}{10} \xi\right) \right] (lk_m - \frac{11}{91} \pi) (3e^{-2\xi} \\ & \times \left\{ 16lk_m \xi^2 (e^{2\xi} - 1) + \pi^3 [1 - e^{2\xi} + 2\xi(1 + \xi)] \right\}) \end{aligned} \quad (87)$$

or, written differently,

$$\begin{aligned} \alpha_7 = & -\frac{1}{9} \pi^2 (24m - \pi^2)^{-1} ml^{-2} \delta^2 \xi^{-3} M_b^{-2} \\ & \times \left[ \frac{21}{32} + \frac{19}{56} \exp\left(-\frac{27}{10} \xi\right) \right] \left( m - \frac{11}{91} \right) \\ & \left( 3e^{-2\xi} \left\{ 16m \xi^2 (e^{2\xi} - 1) + \pi^2 [1 - e^{2\xi} + 2\xi(1 + \xi)] \right\} \right) \end{aligned} \quad (88)$$

## H. Eighth Factor: Pseudo Acoustic Correction

The last two terms are due to the coupling between the pseudo pressure associated with the vortical field and either the unsteady acoustical or rotational velocities. The first term can be expressed by

$$\alpha_8 = E_m^{-2} e^{-2\alpha_m t} \iiint_V \langle -\hat{\mathbf{u}} \cdot \nabla \tilde{p} \rangle dV \quad (89)$$

Following the form usual,<sup>37</sup> one writes

$$\tilde{p} = \exp(\alpha_m t) \left[ \tilde{p}_m^r \cos(k_m t) + \tilde{p}_m^i \sin(k_m t) \right] \quad (90)$$

where

$$\begin{aligned} \tilde{p}_m^r = & -\frac{1}{2} \pi M_b z \sin(\psi) \sin(\eta) \cos(\eta) \\ & \times \exp(\phi) \sin[k_m z \cos(\eta)] \end{aligned} \quad (91)$$

and

$$\begin{aligned} \tilde{p}_m^i = & \frac{1}{2} \pi M_b z \cos(\psi) \sin(\eta) \cos(\eta) \\ & \times \exp(\phi) \sin[k_m z \cos(\eta)] \end{aligned} \quad (92)$$

Accordingly,

$$\nabla \tilde{p} = \exp(\alpha_m t) \left[ \cos(k_m t) \nabla \tilde{p}_m^r + \sin(k_m t) \nabla \tilde{p}_m^i \right] \quad (93)$$

where

$$\begin{aligned} \nabla \tilde{p}_m^r = & \frac{\partial}{\partial y} (\tilde{p}_m^r) \mathbf{e}_y + \frac{\partial}{\partial z} (\tilde{p}_m^r) \mathbf{e}_z \\ = & -\frac{1}{2} \pi (k_m / U_y) z \cos(\psi) \sin(\eta) \cos(\eta) \exp(\phi) \\ & \times \sin[k_m z \cos(\eta)] \mathbf{e}_y - \frac{1}{2} \pi M_b \sin(\psi) \sin(\eta) \cos(\eta) \exp(\phi) \\ & \times \left\{ \sin[k_m z \cos(\eta)] + k_m z \cos(\eta) \cos[k_m z \cos(\eta)] \right\} \mathbf{e}_z \end{aligned} \quad (94)$$

and

$$\begin{aligned} \nabla \tilde{p}_m^i = & \frac{\partial}{\partial y} (\tilde{p}_m^i) \mathbf{e}_y + \frac{\partial}{\partial z} (\tilde{p}_m^i) \mathbf{e}_z \\ = & -\frac{1}{2} \pi (k_m / U_y) z \sin(\psi) \sin(\eta) \cos(\eta) \exp(\phi) \\ & \times \sin[k_m z \cos(\eta)] \mathbf{e}_y + \frac{1}{2} \pi M_b \cos(\psi) \sin(\eta) \cos(\eta) \exp(\phi) \\ & \times \left\{ \sin[k_m z \cos(\eta)] + k_m z \cos(\eta) \cos[k_m z \cos(\eta)] \right\} \mathbf{e}_z \end{aligned} \quad (95)$$

Before time-averaging, the integrand in  $\alpha_8$  can be expanded into

$$\begin{aligned} \hat{\mathbf{u}} \cdot \nabla \tilde{p} = & \frac{1}{2} \pi M_b \exp(2\alpha_m t) \sin(k_m z) \sin(k_m t) \\ & \times \sin(\eta) \cos(\eta) \exp(\phi) \left\{ \sin[k_m z \cos(\eta)] \right. \\ & \left. + k_m z \cos(\eta) \cos[k_m z \cos(\eta)] \right\} [\cos(\psi) \\ & \times \sin(k_m t) - \sin(\psi) \cos(k_m t)] \end{aligned} \quad (96)$$

hence,

$$\begin{aligned} \langle \hat{\mathbf{u}} \cdot \nabla \tilde{p} \rangle = & \frac{1}{4} \pi M_b \exp(2\alpha_m t) \sin(k_m z) \sin(\eta) \\ & \cos(\eta) \exp(\phi) \cos(\psi) \left\{ \sin[k_m z \cos(\eta)] \right. \\ & \left. + k_m z \cos(\eta) \cos[k_m z \cos(\eta)] \right\} \end{aligned} \quad (97)$$

The corresponding integral becomes

$$\begin{aligned} \alpha_8 = & -\frac{1}{4} \pi M_b E_m^{-2} \iiint_V \exp(\phi) \sin(k_m z) \sin(\eta) \cos(\eta) \cos(\psi) \\ & \times \left\{ \sin[k_m z \cos(\eta)] + k_m z \cos(\eta) \cos[k_m z \cos(\eta)] \right\} dV \end{aligned} \quad (98)$$

This can be evaluated from

$$\begin{aligned} \alpha_8 = & -\frac{1}{2} \pi M_b E_m^{-2} \int_0^w \int_0^l \int_0^1 \sin(k_m z) \sin(\eta) \cos(\eta) e^\phi \cos(\psi) \\ & \times \left\{ \sin[k_m z \cos(\eta)] + k_m z \cos(\eta) \cos[k_m z \cos(\eta)] \right\} dy dz dx \end{aligned}$$

$$= -\frac{1}{2}\pi w M_b E_m^{-2} \int_0^l \int_0^1 \sin(k_m z) \sin(\eta) \cos(\eta) e^\phi \cos(\psi) + \{1 + z k_m \cos(\eta) \cot[k_m z \cos(\eta)]\} \quad (106)$$

$$\times \left\{ \sin[k_m z \cos(\eta)] + k_m z \cos(\eta) \cos[k_m z \cos(\eta)] \right\} dy dz \quad (99)$$

At this juncture, one can directly integrate Eq. (99) with respect to  $z$ . The outcome is

$$\alpha_8 = -\frac{1}{2}\pi w M_b E_m^{-2} \int_0^1 Q(y) dy \quad (100)$$

where

$$\begin{aligned} Q(y) &= \frac{1}{64k_m} \exp(\phi) \cos(\psi) \sin(\eta) \cos(\eta) \\ &\left( \{ l k_m \cos(\eta) \cos[k_m l \cos(\eta)] \csc^4\left(\frac{1}{4}\pi y\right) \sec^4\left(\frac{1}{4}\pi y\right) \right. \\ &\times \left. \left[ \cos(lk_m - \pi y) + \cos(lk_m + \pi y) - 2 \cos(lk_m) \right] \right\} \\ &+ \frac{1}{4} \left\{ \csc^4\left(\frac{1}{4}\pi y\right) \sec^4\left(\frac{1}{4}\pi y\right) [lk_m \sin(lk_m - 2\pi y) \right. \\ &+ lk_m \sin(lk_m + 2\pi y) - 24 \cos(lk_m) - 4 \cos(lk_m - \pi y) \\ &\left. - 4 \cos(lk_m + \pi y)] \sin[k_m l \cos(\eta)] \right\} \quad (101) \end{aligned}$$

The result must then be linearized and integrated with respect to  $y$ . One obtains

$$\begin{aligned} \alpha_8 &\approx -\frac{1}{2} w \pi M_b E_m^{-2} \int_0^1 \exp(-\xi y) \cos(k_m y / M_b) \\ &\times \left\{ \frac{1}{8} l \pi y + y^3 \left[ -\frac{1}{48} l \pi^3 + \frac{1}{2} \pi \left( \frac{1}{60} l \pi^2 - \frac{1}{96} \pi^2 l^3 k_m^2 + \dots \right) \right] \right\} dy \quad (102) \end{aligned}$$

and so

$$\alpha_8 = -\frac{1}{16} w \pi^2 l M_b^3 E_m^{-2} \left( \xi^2 M_b^2 - k_m^2 \right) \left( \xi^2 M_b^2 + k_m^2 \right)^{-2} \quad (103)$$

This can be rearranged into

$$\begin{aligned} \alpha_8 &= \frac{-1}{18} \pi^2 M_b^3 \left( \xi^2 M_b^2 - m^2 \pi^2 l^{-2} \right) \\ &\times \left( \xi^2 M_b^2 + m^2 \pi^2 l^{-2} \right)^{-2} \quad (104) \end{aligned}$$

### I. Ninth Factor: Pseudo Vorticity Correction

The last term is due to the less obvious coupling that is formed between vorticity-induced pseudo pressure and the unsteady rotational velocity. The significance of this term can be derived from

$$\alpha_9 = -E_m^{-2} e^{-2\alpha_m t} \iiint_V \langle \tilde{\mathbf{u}} \cdot \nabla \tilde{p} \rangle dV \quad (105)$$

One carries out the time-averaging to obtain

$$\begin{aligned} \langle \tilde{\mathbf{u}} \cdot \nabla \tilde{p} \rangle &= -\frac{1}{4} \pi M_b \exp(2\alpha_m t) \exp(2\phi) \cos^2(\eta) \\ &\times \sin(\eta) \sin^2[k_m z \cos(\eta)] (k_m z \cos(\eta) \cot[k_m z \cos(\eta)]) \end{aligned}$$

The volumetric integral becomes

$$\begin{aligned} \alpha_9 &= \frac{1}{4} \pi M_b E_m^{-2} \iiint_V \exp(2\phi) \cos^2(\eta) \sin(\eta) \sin^2 \\ &\times [k_m z \cos(\eta)] (k_m z \cos(\eta) \cot[k_m z \cos(\eta)] + \{1 \\ &+ z k_m \cos(\eta) \cot[k_m z \cos(\eta)]\}) dV \quad (107) \end{aligned}$$

and so,

$$\begin{aligned} \alpha_9 &= \frac{1}{2} \pi w M_b E_m^{-2} \int_0^l \int_0^1 \exp(2\phi) \cos^2(\eta) \sin(\eta) \\ &\times \sin^2[k_m z \cos(\eta)] (k_m z \cos(\eta) \cot[k_m z \cos(\eta)] \\ &+ \{1 + z k_m \cos(\eta) \cot[k_m z \cos(\eta)]\}) dy dz \quad (108) \end{aligned}$$

Next, the integral with respect to  $z$  is evaluated. The subsequent expression is transformed into  $y$ , linearized near the wall, and integrated term-by-term. After some effort, one finds

$$\begin{aligned} \alpha_9 &= \frac{1}{2} \pi w l M_b E_m^{-2} \int_0^1 \exp(2\phi) \cos^2(\eta) \\ &\times \sin(\eta) \sin^2[k_m z \cos(\eta)] dy \quad (109) \end{aligned}$$

Equation (109) requires an asymptotic treatment that relies, in part, on trigonometric identities. One collects

$$\alpha_9 = \frac{1}{2} \frac{\pi w l}{M_b^{-1} E_m^2} \int_0^1 \left( \frac{1}{2} \pi y - \frac{7}{48} \pi^3 y^3 + \frac{61}{3840} \pi^5 y^5 + \dots \right) dy \quad (110)$$

which, at length, gives

$$\begin{aligned} \alpha_9 &= \frac{1}{6} w l M_b E_m^{-2} \left( 1 - \frac{3}{2} \pi^{-2} \right) \left( \frac{427}{425} + \frac{917}{374} \xi + \frac{95}{61} \xi^2 + \frac{437}{670} \xi^3 \right. \\ &\left. + \frac{101}{847} \xi^4 + \frac{1}{65} \xi^5 + \frac{1}{794} \xi^6 \right)^{-1} \quad (111) \end{aligned}$$

otherwise, one can put

$$\begin{aligned} \alpha_9 &= \frac{4}{27} M_b \left( 1 - \frac{3}{2} \pi^{-2} \right) \left( \frac{427}{425} + \frac{917}{374} \xi + \frac{95}{61} \xi^2 + \frac{437}{670} \xi^3 \right. \\ &\left. + \frac{101}{847} \xi^4 + \frac{1}{65} \xi^5 + \frac{1}{794} \xi^6 \right)^{-1} \quad (112) \end{aligned}$$

### J. Tenth Factor: Unsteady Nozzle Correction

The tenth correction factor in stability calculations is due to the unsteady rotational energy crossing the motor exit plane. This growth rate is precipitated by the third and fourth rotational terms; these can be lumped together into

$$\alpha_{10} = -M_b E_m^{-2} e^{-2\alpha_m t} \iiint_V \langle (\hat{\mathbf{u}} + \tilde{\mathbf{u}}) \cdot \nabla (U \cdot \tilde{\mathbf{u}}) \rangle dV \quad (113)$$

This triple integral can be converted into

$$\begin{aligned}\alpha_{10} &= -M_b E_m^{-2} e^{-2\alpha_m t} \iint_{S_N} \langle [\mathbf{n} \cdot (\hat{\mathbf{u}} + \tilde{\mathbf{u}})] (\mathbf{U} \cdot \tilde{\mathbf{u}}) \rangle dS \\ &= -M_b E_m^{-2} e^{-2\alpha_m t} \iint_{S_N} \langle \tilde{u}_z^2 U_z \rangle dS + O(M_b^2)\end{aligned}\quad (114)$$

knowing that

$$\begin{aligned}\tilde{u}_z^2 &= \cos^2(\eta) \sin^2[k_m z \cos(\eta)] \exp(2\phi) e^{2\alpha_m t} \\ &\times [\cos^2 \psi \sin^2(k_m t) + \sin^2 \psi \cos^2(k_m t) \\ &\quad - 2 \cos \psi \sin(k_m t) \sin \psi \cos(k_m t)]\end{aligned}\quad (115)$$

one gets

$$\begin{aligned}\alpha_{10} &= -\frac{1}{2} \pi M_b E_m^{-2} e^{-2\alpha_m t} \iint_{S_N} \langle z \cos^2(\eta) \sin^2[k_m z \cos(\eta)] \\ &\times \exp(2\phi) e^{2\alpha_m t} [\cos^2 \psi \sin^2(k_m t) + \sin^2 \psi \cos^2(k_m t) \\ &\quad - 2 \cos \psi \sin(k_m t) \sin \psi \cos(k_m t)] \sin(\eta) \rangle dS\end{aligned}\quad (116)$$

which, after time-averaging, yields

$$\begin{aligned}\alpha_{10} &= -\frac{1}{4} \pi M_b E_m^{-2} \iint_{S_N} z \exp(2\phi) \cos^2(\eta) \sin(\eta) \\ &\times \sin^2[k_m z \cos(\eta)] dS\end{aligned}\quad (117)$$

and so

$$\begin{aligned}\alpha_{10} &= -\frac{1}{2} \pi l M_b E_m^{-2} \int_0^w \int_0^1 \exp(2\phi) \cos^2(\eta) \sin(\eta) \\ &\times \sin^2[k_m z \cos(\eta)] dy dx\end{aligned}\quad (118)$$

Subsequent integration gives

$$\begin{aligned}\alpha_{10} &= -\frac{1}{2} \pi w l M_b E_m^{-2} \int_0^1 \exp(2\phi) \cos^2(\eta) \sin(\eta) \\ &\times \sin^2[k_m z \cos(\eta)] dy\end{aligned}\quad (119)$$

which can be expressed as

$$\begin{aligned}\alpha_{10} &= -\frac{4}{27} M_b \left(1 - \frac{3}{2} \pi^{-2}\right) \left(\frac{427}{425} + \frac{917}{374} \xi + \frac{95}{61} \xi^2 + \frac{437}{670} \xi^3 \right. \\ &\quad \left. + \frac{101}{847} \xi^4 + \frac{1}{65} \xi^5 + \frac{1}{794} \xi^6\right)^{-1}\end{aligned}\quad (120)$$

A fortuitous and totally unexpected result can be noted in that  $\alpha_{10} = -\alpha_9$ .

## IV. Discussion

### A. Standard Formulation

The degree of improvement associated with the current results may be assessed by comparing the improved predictions with those derived from the standard stability formulation. Again, the characteristic parameters of the four representative cases introduced by Flandro<sup>43</sup> will be used. As indicated earlier, the classical stability formulation does not retain unsteady

rotational effects except through the flow turning term, which was first derived using a one-dimensional representation. The growth rate predicted by the irrotational model consists of

$$\begin{aligned}\alpha_i &= \alpha_{1-4} = -\frac{1}{2} w l M_b E_m^{-2} \gamma_b - \frac{2}{3} w l k_m^2 \delta^2 E_m^{-2} \\ &\quad - \frac{1}{2} w l M_b E_m^{-2} \left(1 + M_b^2 \xi^2 / k_m^2\right)^{-1}\end{aligned}\quad (121)$$

where  $\gamma_b \equiv 2\gamma - (A_b + 1)$ . Recalling that the irrotational energy normalization is given by  $(E_m^2)_i = wL/H$ , Eq. (121) can be put in the form  $\alpha_{1-4} = \frac{1}{2} K_i M_b$ ; the irrotational growth rate coefficient is simply

$$K_i = -\gamma_b - \frac{4}{3} \xi M_b^2 - \left[1 + M_b^2 \xi^2 l^2 / (m^2 \pi^2)\right]^{-1}\quad (122)$$

The sign of  $K_i$  will directly prescribe motor stability. Understanding how  $K_i$  changes sign (e.g. from negative to positive) as  $\xi$  is varied is the key to studying the changes in the stability behavior. This can be best accomplished by examining Cardano's discriminant for  $K_i = 0$ . One finds

$$\begin{aligned}\Delta_i &= 9l^2 (1 + \gamma_b) \gamma_b^3 + m^2 \pi^2 [27 + 16\gamma_b (9 + 4\gamma_b)] M_b^2 \\ &\quad (123)\end{aligned}$$

When  $\Delta_i < 0$ ,  $K_i$  will change sign at the critical damping parameter of

$$\begin{aligned}\xi_i &= \left[ \sqrt{\gamma_b^2 - \frac{16}{3} m^2 \pi^2 M_b^2 l^{-2}} \right. \\ &\times \sin\left(\frac{1}{3} \sin^{-1} \left\{ \left( \gamma_b^2 - \frac{16}{3} m^2 \pi^2 M_b^2 l^{-2} \right)^{-\frac{3}{2}} \left[ \gamma_b^3 \right. \right. \right. \\ &\quad \left. \left. \left. + (24 - 16\gamma_b) m^2 \pi^2 M_b^2 l^{-2} \right] \right\} \right) - \frac{1}{2} \gamma_b \left. \right] / (2M_b^2)\end{aligned}\quad (124)$$

It may be instructive to note that whenever  $\gamma_b < -1$ ,  $K_i$  will be negative, hence indicating a stable system. Also when  $\gamma_b > 0$ ,  $K_i$  will be positive, hence indicating an unstable one. However, when  $\Delta_i < 0$ , an unstable system is realized for  $\xi > \xi_i$ ; it appears that the irrotational formulation is missing an important element so long as friction has a damping rather than an energizing effect. Physically, increasing  $\xi$  at a given oscillation mode number (beyond some critical value) should have a stabilizing impact because it can only be accomplished by increasing the dimensionless viscosity  $\delta$ , decreasing the surface Mach number, or decreasing the length of the motor. Any of these changes should lead to a more stable system.

Another way of assessing the stability of the system is by examining the other critical values of key parameters which may cause the system to cross from stability to instability and vice versa. After some algebra, one finds

$$M_b^* = \left(8\xi^2 l^2\right)^{-\frac{1}{2}} \left[-3\gamma_b \xi l^2 - 4m^2 \pi^2 + \left(9\gamma_b^2 \xi^2 l^4 + 16m^4 \pi^4 - 24\gamma_b \xi l^2 m^2 \pi^2 - 48\xi \pi^2 m^2 l^2\right)^{\frac{1}{2}}\right]^{\frac{1}{2}} \quad (125)$$

to be the critical value of the injection Mach number. Moreover one can proceed to find

$$l^* = \left[-\left(\gamma_b + \frac{4}{3}\xi M_b^2 + 1\right)\left(\gamma_b + \frac{4}{3}\xi M_b^2\right)^{-1} \times m^2 \pi^2 \xi^{-2} M_b^{-2}\right]^{\frac{1}{2}} \quad (126)$$

to be the critical characteristic length of the slab motor that will cause a change in the stability status of a given system. As such it can be determined that whenever  $M_b < M_b^*$ , or  $l > l^*$  the system becomes unstable. Note that  $l^*$  is unphysical, being purely imaginary.

### B. Improved Linear Formulation

For a more precise stability estimation, one must involve all available rotational interactions. This can be accomplished by taking

$$\alpha_r = \alpha_{1-10} = \sum_{n=1}^{10} \alpha_n \quad (127)$$

where the corrected energy normalization is based on<sup>44</sup>

$$(E_m^2)_r = \frac{9}{8} \pi L / H \quad (128)$$

The superposition of these terms gives  $\alpha_{1-10} = \frac{4}{9} M_b K_r$ ; the rotational stability coefficient is realizable from

$$K_r = C - \frac{4}{3} M_b^2 \xi - \frac{1}{8} \pi^2 M_b^2 \left(\xi^2 M_b^2 - m^2 \pi^2 l^{-2}\right) \times \left(\xi^2 M_b^2 + m^2 \pi^2 l^{-2}\right)^{-2} \quad (129)$$

where

$$C = -\gamma_b + \frac{1}{2} \left\{1 - \frac{1}{24} \left[m \pi^2 \xi^4 e^{2\xi} (\pi^2 - 12)\right]^{-1} \times \left[\frac{39}{85} + \frac{1}{82} \xi + \frac{7}{13} \exp\left(-\frac{107}{50} \xi\right)\right] (4m\pi^2 + 3) \left[(1 + 2\xi - e^{2\xi}) + \pi^2 \left\{3e^{2\xi} - 3 - 2\xi [3 + \xi(3 + 2\xi)]\right\} 12\xi^2\right]\right\} - \frac{1}{4} (m\pi\xi)^{-1} (24m - \pi^2)^{-1} \left[\frac{21}{32} + \frac{19}{56} \exp\left(-\frac{27}{10} \xi\right)\right] \times \left(m\pi - \frac{11}{91}\right) \left\{3\xi^{-1} e^{-2\xi} \left\{16m\xi^2 (e^{2\xi} - 1) + \pi^2 [1 - e^{2\xi} + 2\xi(1 + \xi)]\right\}\right\} \quad (130)$$

Equation (129) enables us to seek direct relations between chamber parameters that will ensure a stable system by guaranteeing a negative  $K_r$ . Similar

relations can be helpful in the developmental stages of motors exhibiting less simplistic grain configurations.

It is worth mentioning at this point that this expression is valid only when  $M_b \leq 0.01$  and  $\xi \leq 1.0$ . These ranges encapsulate the parametric spectrum associated with solid rocket motors.

The complexity of Eq. (130) makes obtaining an analytical expression for the critical value of  $\xi$  infeasible. At this point we will only present the critical values of the other key parameters. One finds

$$M_b^* = \frac{m\pi}{\xi l} \left\{(-\pi^2 + 8C\xi^2)^{-1} \times \left[-\frac{1}{2}\pi^2 - 8C\xi^2 + \frac{1}{2}\pi(\pi^2 + 64C\xi^2)^{\frac{1}{2}}\right]\right\}^{\frac{1}{2}} \quad (131)$$

to be the critical value of the injection Mach number. Moreover, one evaluates the critical value of the slab motor length to be

$$l^* = \frac{m\pi}{\xi M_b} \left\{(-\pi^2 + 8C\xi^2)^{-1} \times \left[-\frac{1}{2}\pi^2 - 8C\xi^2 + \frac{1}{2}\pi(\pi^2 + 64C\xi^2)^{\frac{1}{2}}\right]\right\}^{\frac{1}{2}} \quad (132)$$

It is worth remarking that when  $M_b > M_b^*$ , or  $l > l^*$  the system is unstable. It is stable otherwise.

### C. Comparing Numerics and Asymptotics

Summarized in Tables 1–2 are the results from the irrotational and improved formulations. These dimensional growth rates are related to the non-dimensional values via  $\alpha^* = \alpha a_0 / H$ . In Table 1, all factors are computed by numerically evaluating the volumetric integrals. In Table 2, the analytical expressions derived earlier are used to estimate the corresponding factors. From these tables, one realizes that a significant discrepancy exists between the irrotational prediction  $\alpha_{1-4}^*$  and the rotationally adjusted value  $\alpha_{1-10}^*$ . This discrepancy varies from 36% for the equivalent Cold-Flow Experiment to about 111% for the equivalent (slab-scaled) Small Rocket Motor. Again, the latter discrepancy suggests a less stable system than projected by conventional theory. Clearly, the additional rotational corrections play an essential role in the proper assessment of instability.

Comparing numerical results from Table 1 to analytical ones from Table 2, one can discern the excellent capability of analytical approximations to reproduce the numerically integrated growth rate factors. The encountered error varies from 0% in the equivalent RSRM configuration, to about 1.32% in the equivalent Tactical Rocket. Due to their asymptotic nature, the analytical expressions can be substituted for

**Table 1 Numerical integrals of classic, improved, and individual growth rates (sec<sup>-1</sup>)**

Motor	$\alpha_{1-4}^*$ <sup>a</sup> classic	$\alpha_{1-10}^*$ improved	$ \Delta\alpha/\alpha \%$	$\alpha_1^*$	$\alpha_2^*$	$\alpha_4^*$	$\alpha_5^*$	$\alpha_6^*$	$\alpha_7^*$	$\alpha_8^*$	$\alpha_9^*$	$\alpha_{10}^*$
Small	-0.15	44.19	100	40.0	-18.0 <sup>-5</sup>	-40.2	40.2	19.5	-15.3	925 <sup>-5</sup>	2.02	-2.02
Tactical	-31.1	-2.27	92.7	-7.90	-1.59 <sup>-5</sup>	-19.7	19.7	6.61	-0.987	939 <sup>-5</sup>	4.79	-4.79
Cold Flow	-43.2	-27.84	35.6	-30.1	-10.6 <sup>-6</sup>	-8.28	8.28	2.84	-0.565	0.0130	1.92	-1.92
Space	-3.60	-0.56	84.4	-1.20	-4.92 <sup>-8</sup>	-2.00	2.00	0.644	-0.006	0.0033	0.558	-0.558

<sup>a</sup>The sum of the growth rates is multiplied by 9/8 to be consistent with the standard stability formulation based on an energy normalization value of  $(E_m^2)_i = WL/H$  instead of  $(E_m^2)_r = (9/8)WL/H$ .

**Table 2 Analytical estimates of classic, improved, and individual growth rates (sec<sup>-1</sup>)**

Motor	$\alpha_{1-4}^*$ <sup>a</sup> classic	$\alpha_{1-10}^*$ improved	$ \Delta\alpha/\alpha \%$	$\alpha_1^*$	$\alpha_2^*$	$\alpha_4^*$	$\alpha_5^*$	$\alpha_6^*$	$\alpha_7^*$	$\alpha_8^*$	$\alpha_9^*$	$\alpha_{10}^*$
Small	-4.88	43.89	111	40.0	-18.0 <sup>-5</sup>	-44.4	44.4	19.4	-15.5	925 <sup>-5</sup>	2.02	-2.02
Tactical	-31.1	-2.24	92.8	-7.90	-1.59 <sup>-5</sup>	-19.8	19.8	6.62	-0.975	939 <sup>-5</sup>	4.79	-4.79
Cold Flow	-43.3	-27.82	35.8	-30.1	-10.6 <sup>-6</sup>	-8.04	8.04	2.85	-0.558	0.0130	1.92	-1.92
Space	-3.61	-0.56	84.5	-1.20	-4.92 <sup>-8</sup>	-2.01	2.01	0.643	-0.006	0.0033	0.560	-0.560

rather costly numerical simulations in the domain where the values of  $\xi \leq 1.0$  and  $M_b \leq 0.01$ . This restriction will ensure that the asymptotic approximations used in perturbing the respective growth rate expressions remain valid. The corresponding physical range is in fact quite appropriate of practical motor chamber conditions.

Tables 1 and 2 can be used to assess the order of magnitude of various growth rates. The largest contributors can be readily identified to be pressure coupling, flow turning, rotational flow, mean vorticity, viscosity, pseudo vorticity, and unsteady nozzle corrections. Conversely, the dilatational energy, acoustic mean flow, and pseudo acoustic corrections are either vanishingly or negligibly small. Due to intermediate cancellations, only pressure coupling, mean vorticity and viscosity corrections survive in the overall assessment. These must of course be supplemented by corrections due to particle damping, distributed combustion, and two-phase interactions.

#### D. Growth Rate Sensitivity

An integral part of assessing the acoustic instability growth in SRMs rests in understanding the role that the various working parameters play in this process. To that end, a number of illustrations presented subsequently in this section will describe the effect of varying the key parameters in a fashion that reproduces different operational settings. A careful analysis of these illustrations will further serve to validate the

mathematical model as current results will be shown to follow correct physical predictions.

Figure 2 is devoted to showing the stability predictions based on the irrotational formulation in contrast to those based on an improved formulation presented in this study. In Figs. 2a and 2b, numerical stability growth rates based on the current formulation are plotted versus the viscous parameter for several injection Mach numbers. It is clear that the plots generally follow the physical predictions corroborated by the asymptotic solutions; for example, one notes that an increase in  $\xi$  at constant  $M_b$  promotes system stability. Conversely, an increase in  $M_b$  at constant  $\xi$  is destabilizing.

By comparing Fig. 2a and 2b, one can identify the role of viscous friction to be rather unimportant in short motors (for example, when  $L/H = 20$ ); it becomes more appreciable, however, as the length is increased (in Fig. 2b where  $L/H = 50$ ). This result may be ascribed to the longer residence time and trajectory of particles in longer chambers.

Figure 2c displays numerical stability growth rates based on the irrotational formulation as function of the viscous parameter. Note that the trends associated with the irrotational model contradict almost categorically the physical predictions in this case. Figure 2c demonstrates the tendency for the system to become less stable as the viscosity of the fluid is increased. Moreover, a decrease in  $M_b$  at constant  $\xi$  appears to be destabilizing. Both trends are unphysical. The clear

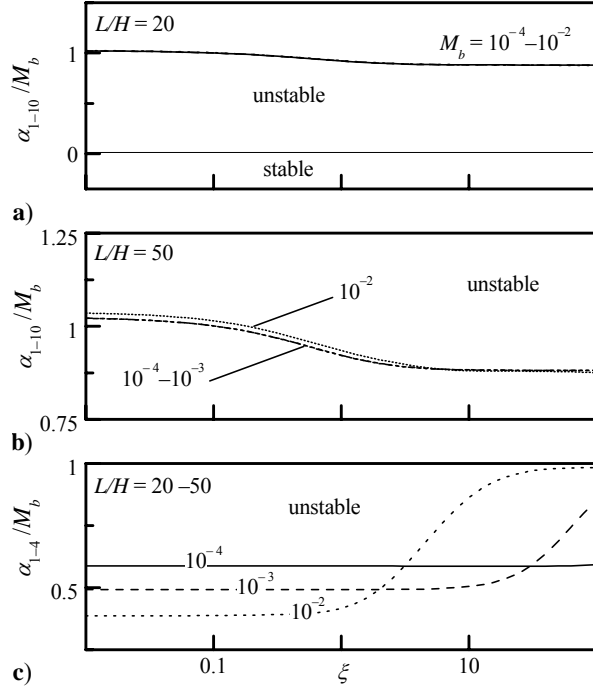


**Fig. 2** Numerical stability curves at constant  $M_b$  shown over a useful range of  $\xi$  and select values of  $L/H$ . The system is more sensitive to the stabilizing role of  $\xi$  at higher  $L/H$  and  $M_b$ . Here  $A_b^{(r)} = 1.75$ ,  $\gamma = 1.3$ , and  $m = 1$ .

shortcomings of the irrotational approach in predicting acoustic stability in SRMs (and which was noted by Flandro and Majdalani<sup>37</sup>) is seen to be recurrent in the slab motor configuration.

This important observation is further reinforced by the results given in Fig. 3. An increase in  $\delta$  at constant injection Mach number and motor length (thus an increase in  $\xi$ ) is shown to predict a more stable system in Figs. 3a and 3b. The improved stability formulation proves consistent with the physically stabilizing nature of friction. This is not the case in Figs. 3c and 3d which depict the numerical stability curves based on the one-dimensional formulation. Using the irrotational model, the system grows sharply unstable as viscosity, a salient stability ingredient, is increased.

## V. Concluding Remarks

By incorporating the total kinetic energy of the unsteady rotational disturbances into the energy density equation, a more inclusive and physically meaningful assessment of acoustic instability factors has been demonstrated here for the slab rocket motor. The new framework is shown to offer critical advantages over the classic formulation which was formerly based on an

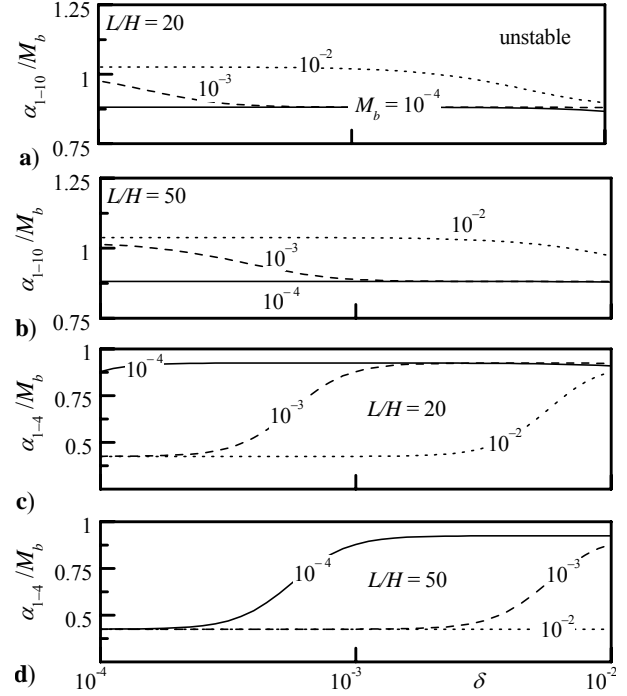


**Fig. 3** Numerical stability curves at constant  $M_b$  shown over a useful range of  $\delta$  and select values of  $L/H$ . The rotational formulation predicts a less stable system when  $\delta$  is lowered or when  $L/H$  or  $M_b$  are increased. This explains, in part, the additional instabilities observed in elongated motors. The standard irrotational formulation predicts the opposite trends. Here  $\gamma = 1.3$  and  $m = 1$ .

irrotational representation of the acoustic field. The new formulation gives rise to six additional growth rate terms that have been discounted in irrotational stability models. These include corrections owing to the rotational flow, mean vorticity, viscosity, pseudo acoustic, pseudo vorticity, and unsteady nozzle effects. These are summarized in Table 3 in both general and asymptotic forms, including the original corrections evolving from one-dimensional wave theory. The new terms are precipitated, no doubt, from the unsteady rotational disturbances and their interactions with the acoustic wave motion. Interestingly, the rotational flow and unsteady nozzle corrections are identically equal but opposite in sign to the flow turning and pseudo vorticity corrections, respectively. At the outset, three linear growth rates survive the attendant cancellations. These are pressure coupling, mean vorticity, and viscosity corrections.

From a physical standpoint, the cancellation of flow turning by another term is gratifying. In fact, it confirms the 1982 mathematical proof offered by Van

**Table 3 Asymptotic growth rate corrections for the slab motor**

	Improved rotational set in general form	Evaluated growth rates (dimensionless)
	$E_m^2 = \frac{1}{2} \iiint_V [(\hat{p}_m)^2 + \hat{\mathbf{u}}_m \cdot \hat{\mathbf{u}}_m + 2\hat{\mathbf{u}}_m \cdot \hat{\mathbf{u}}_m^i + \hat{\mathbf{u}}_m^i \cdot \hat{\mathbf{u}}_m^i + \hat{\mathbf{u}}_m^i \cdot \hat{\mathbf{u}}_m^i] dV$	
$\alpha_1$ : Pressure coupling	$-E_m^{-2} \exp(-2\alpha_m t) \iiint_V \left\langle \nabla \cdot \left[ \hat{p} \hat{\mathbf{u}} + \frac{1}{2} M_b \mathbf{U} (\hat{p})^2 \right] + M_b [\hat{\mathbf{u}} \cdot \nabla (\mathbf{U} \cdot \hat{\mathbf{u}})] \right\rangle dV$	$\frac{4}{9} M_b [(A_b^{(r)} + 1) - 2\gamma]$
$\alpha_2$ : Dilatational	$E_m^{-2} \exp(-2\alpha_m t) \iiint_V \left\langle \frac{4}{3} \delta^2 \hat{\mathbf{u}} \cdot \nabla (\nabla \cdot \hat{\mathbf{u}}) \right\rangle dV$	$-\frac{5}{8} \xi M_b^3 \ll O(1)$
$\alpha_3$ : Acoustic mean	$E_m^{-2} \exp(-2\alpha_m t) \iiint_V \left\langle M_b \hat{\mathbf{u}} \cdot (\hat{\mathbf{u}} \times \boldsymbol{\Omega}) \right\rangle dV$	0
$\alpha_4$ : Flow turning	$E_m^{-2} \exp(-2\alpha_m t) \iiint_V \left\langle M_b \hat{\mathbf{u}} \cdot (\mathbf{U} \times \boldsymbol{\omega}) \right\rangle dV$	$-\frac{4}{9} M_b (1 + \pi^{-2} M_b^2 \xi^2 l^2 m^{-2})^{-1}$
$\alpha_5$ : Rotational flow	$-E_m^{-2} \exp(-2\alpha_m t) \iiint_V \left\langle \tilde{\mathbf{u}} \cdot \nabla \hat{p} \right\rangle dV$	$\frac{4}{9} M_b (1 + \pi^{-2} M_b^2 \xi^2 l^2 m^{-2})^{-1}$
$\alpha_6$ : Mean vorticity	$E_m^{-2} \exp(-2\alpha_m t) \iiint_V \left\langle M_b \tilde{\mathbf{u}} \cdot (\mathbf{U} \times \boldsymbol{\omega}) \right\rangle dV$	$\frac{2}{9} M_b \left\{ 1 - \frac{1}{24} \left[ m \pi^2 \xi^4 e^{2\xi} (\pi^2 - 12) \right]^{-1} \right.$ $\times \left[ \frac{39}{85} + \frac{1}{82} \xi + \frac{7}{13} \exp\left(-\frac{107}{50} \xi\right) \right] (4m\pi^2 + 3) (12\xi^2$ $\times (1 + 2\xi - e^{2\xi}) + \pi^2 \{ 3e^{2\xi} - 3 - 2\xi [3 + \xi(3 + 2\xi)] \} \left. \right\}$
$\alpha_7$ : Viscosity	$-E_m^{-2} \exp(-2\alpha_m t) \iiint_V \left\langle \delta^2 (\hat{\mathbf{u}} + \tilde{\mathbf{u}}) \cdot (\nabla \times \boldsymbol{\omega}) \right\rangle dV$	$-\frac{1}{9} \pi^2 (24m - \pi^2)^{-1} m l^{-2} \delta^2 \xi^{-3} M_b^{-2}$ $\times \left[ \frac{21}{32} + \frac{19}{56} \exp\left(-\frac{27}{10} \xi\right) \right] \left( m - \frac{11}{91} \right)$ $\times \left( 3e^{-2\xi} \{ 16m\xi^2 (e^{2\xi} - 1) + \pi^2 [1 - e^{2\xi} + 2\xi(1 + \xi)] \} \right)$
$\alpha_8$ : Pseudo acoustic	$E_m^{-2} \exp(-2\alpha_m t) \iiint_V \left\langle -\hat{\mathbf{u}} \cdot \nabla \tilde{p} \right\rangle dV$	$\frac{2}{5} M_b^3 l^2 / m^2 \ll O(1)$
$\alpha_9$ : Pseudo vorticity	$-E_m^{-2} \exp(-2\alpha_m t) \iiint_V \left\langle \tilde{\mathbf{u}} \cdot \nabla \tilde{p} \right\rangle dV$	$\frac{4}{27} M_b \left( 1 - \frac{3}{2} \pi^{-2} \right) \left( \frac{427}{425} + \frac{917}{374} \xi + \frac{95}{61} \xi^2 + \frac{437}{670} \xi^3 \right.$ $\left. + \frac{101}{847} \xi^4 + \frac{1}{65} \xi^5 + \frac{1}{794} \xi^6 \right)^{-1}$
$\alpha_{10}$ : Unsteady nozzle	$-E_m^{-2} \exp(-2\alpha_m t) \iiint_V \left\langle M_b (\hat{\mathbf{u}} + \tilde{\mathbf{u}}) \cdot \nabla (\mathbf{U} \cdot \tilde{\mathbf{u}}) \right\rangle dV$	$-\frac{4}{27} M_b \left( 1 - \frac{3}{2} \pi^{-2} \right) \left( \frac{427}{425} + \frac{917}{374} \xi + \frac{95}{61} \xi^2 + \frac{437}{670} \xi^3 \right.$ $\left. + \frac{101}{847} \xi^4 + \frac{1}{65} \xi^5 + \frac{1}{794} \xi^6 \right)^{-1}$

Moorhem;<sup>45</sup> in his well-known analysis, Van Moorhem is able to demonstrate that flow turning, which stems from the need to satisfy fundamental conservation laws in a chamber with sidewall mass addition, is a needed adjustment only if a problem is formulated in one dimensional space. In multi-dimensional settings, such as those employed in most current investigations, flow turning is proven to be absent. Van Moorhem's proof is corroborated here.

The second interesting cancellation is that of pseudo vorticity by virtue of the unsteady nozzle damping. Here too, the outcome brings the results to a closer agreement with conventional theory; the latter downplays the role of the pseudo pressure (or pseudo sound) in the overall energy assessment. In our problem, the only remaining term due to the pseudo

pressure is  $\alpha_8$ , which is indeed very small and, hence, negligible.

As usual, using the four representative motor properties to define four case studies, the improvements in prediction capability are quantified and shown to be quite substantial when compared to the irrotational estimates. The analytical expressions presented here for the slab rocket motor are also shown to provide expeditious approximations for the volume integrals that arise in the stability calculations. Generally, the error in the analytical prediction is shown to differ from the numerical solution by a percent or less.

The analytical expressions also lead to explicit relations between the salient flow attributes and stability. This permits calculating critical motor lengths and Mach numbers that must not be exceeded if hoping

to mitigate acoustic instabilities. Physically, the proposed formulation confirms experimental findings by projecting a less stable environment in longer motors, at higher surface Mach numbers, and for propellants exhibiting higher surface admittance values. In the same vein, a more stable environment is promoted at higher oscillation mode numbers (which absorb more trigger energy) and at increasing levels of viscous damping. The role of the latter becomes more appreciable in longer motors or at higher Mach numbers. Unsurprisingly, both irrotational and rotational relations agree on the role of surface admittance, but seem to be conflicting on most other counts. For this reason, our study suggests the important physical need to incorporate all rotational corrections in future stability calculations.

In recent years, the slab motor geometry has increased in popularity, especially, in academic studies of acoustic instability. The current results are hoped to supplement the existing literature and serve as a benchmark for next generation numerical experiments; additional corrections for the slab motor need to be assessed, and these are hoped to be unraveled in forthcoming investigations. Among instability contributors omitted here are corrections due to time-dependence of the mean pressure, particle damping and multiphase interactions, distributed combustion, parietal vortex shedding (PVS), and intrinsic mean flow instabilities that have been recently reported by Lupoglazoff and Vuillot,<sup>46,47</sup> and Griffond and Casalis.<sup>5,6</sup> It is speculated that such instabilities may appear even in the absence of protrusions, baffles, inhibitors, or inter-segmental gaps. The instability discussed by Griffond and Casalis<sup>5,6</sup> appears to be a property of the mean flow itself and may need to be separately accounted for in the overall energy balance. For each of these factors, additional work lies ahead.

### Acknowledgments

This project was sponsored partly by the University of Tennessee, and partly by the Faculty Early Career Development (CAREER) Program of the National Science Foundation, under Grant No. CMS-0353518. The authors wish to express their grateful appreciation for the support and encouragement received from Dr. Masayoshi Tomizuka, NSF Program Director, Dynamic Systems and Control (CMS). Additionally, the authors wish to thank Dr. Jonathan C. French for his valuable contributions to this project. The authors are equally indebted to the synergistic activities promoted by Dr. Fred S. Blomshield, Head of Combustion and Propulsion Research at the Naval Air Warfare Center; his genuine and abiding interest in acoustic instability research is most gratefully acknowledged.

### References

- <sup>1</sup>Brownlee, W. G., "Nonlinear Axial Combustion Instability in Solid Propellant Motors," *AIAA Journal*, Vol. 2, No. 2, 1964, pp. 275-284.
- <sup>2</sup>Brownlee, W. G., "An Experimental Investigation of Unstable Combustion in Solid Propellant Rocket Motors," Ph.D. Dissertation, California Institute of Technology, 1959.
- <sup>3</sup>Brownlee, W. G., and Marble, F. E., "An Experimental Investigation of Unstable Combustion in Solid Propellant Rocket Motors," *ARS Progress in Astronautics and Rocketry: Solid Propellant Rocket Research*, Vol. 1, edited by M. Summerfield, Academic Press Inc., New York, 1960, pp. 455-494.
- <sup>4</sup>Casalis, G., Avalon, G., and Pineau, J.-P., "Spatial Instability of Planar Channel Flow with Fluid Injection through Porous Walls," *The Physics of Fluids*, Vol. 10, No. 10, 1998, pp. 2558-2568.
- <sup>5</sup>Griffond, J., and Casalis, G., "On the Nonparallel Stability of the Injection Induced Two-Dimensional Taylor Flow," *The Physics of Fluids*, Vol. 13, No. 6, 2001, pp. 1635-1644.
- <sup>6</sup>Griffond, J., and Casalis, G., "On the Dependence on the Formulation of Some Nonparallel Stability Approaches Applied to the Taylor Flow," *The Physics of Fluids*, Vol. 12, No. 2, 2000, pp. 466-468.
- <sup>7</sup>Avalon, G., Casalis, G., and Griffond, J., "Flow Instabilities and Acoustic Resonance of Channels with Wall Injection," AIAA Paper 98-3218, July 1998.
- <sup>8</sup>Liou, T. M., Lien, W. Y., and Hwang, P. W., "Large-Eddy Simulations of Turbulent Reacting Flows in a Chamber with Gaseous Ethylene Injecting through the Porous Wall," *Combustion and Flame*, Vol. 99, No. 3-4, 1994, pp. 591-600.
- <sup>9</sup>Liou, T. M., Lien, W. Y., and Hwang, P. W., "Transition Characteristics of Flowfield in a Simulated Solid-Rocket Motor," *Journal of Propulsion and Power*, Vol. 14, No. 3, 1998, pp. 282-289.
- <sup>10</sup>Liou, T.-M., and Lien, W.-Y., "Numerical Simulations of Injection-Driven Flows in a Two-Dimensional Nozzleless Solid-Rocket Motor," *Journal of Propulsion and Power*, Vol. 11, No. 4, 1995, pp. 600-606.
- <sup>11</sup>Apte, S., and Yang, V., "Unsteady Flow Evolution in a Porous Chamber with Surface Mass Injection. Part I: Free Oscillation," *AIAA Journal*, Vol. 39, No. 8, 2001, pp. 1577-1586.
- <sup>12</sup>Apte, S., and Yang, V., "Unsteady Flow Evolution in a Porous Chamber with Surface Mass Injection. Part



II: Acoustic Excitation,” *AIAA Journal*, Vol. 40, No. 2, 2002, pp. 244-253.

<sup>13</sup>Chu, W.-W., Yang, V., and Majdalani, J., “Premixed Flame Response to Acoustic Waves in a Porous-Walled Chamber with Surface Mass Injection,” *Combustion and Flame*, Vol. 133, No. 6129, 2003, pp. 359-370.

<sup>14</sup>Barron, J., Majdalani, J., and Van Moorhem, W. K., “A Novel Investigation of the Oscillatory Field over a Transpiring Surface,” *Journal of Sound and Vibration*, Vol. 235, No. 2, 2000, pp. 281-297.

<sup>15</sup>Ma, Y., Van Moorhem, W. K., and Shorthill, R. W., “Innovative Method of Investigating the Role of Turbulence in the Velocity Coupling Phenomenon,” *Journal of Vibration and Acoustics-Transactions of the ASME*, Vol. 112, No. 4, 1990, pp. 550-555.

<sup>16</sup>Ma, Y., Van Moorhem, W. K., and Shorthill, R. W., “Experimental Investigation of Velocity Coupling in Combustion Instability,” *Journal of Propulsion and Power*, Vol. 7, No. 5, 1991, pp. 692-699.

<sup>17</sup>Majdalani, J., and Van Moorhem, W. K., “Laminar Cold-Flow Model for the Internal Gas Dynamics of a Slab Rocket Motor,” *Journal of Aerospace Science and Technology*, Vol. 5, No. 3, 2001, pp. 193-207.

<sup>18</sup>Majdalani, J., Barron, J., and Van Moorhem, W. K., “Inception of Turbulence in the Stokes Boundary Layer over a Transpiring Wall,” *ASME Journal of Fluids Engineering*, Vol. 124, No. 9, 2002, pp. 1-7.

<sup>19</sup>Wasistho, B., Haselbacher, A., Najjar, F. M., Tafti, D., Balachandar, S., and Moser, R. D., “Direct and Large Eddy Simulations of Compressible Wall-Injection Flows in Laminar, Transitional, and Turbulent Regimes,” AIAA Paper 2002-4344, July 2002.

<sup>20</sup>Vuillot, F., and Lupoglazoff, N., “Combustion and Turbulent Flow Effects in 2-D Unsteady Navier-Stokes Simulations of Oscillatory Rocket Motors,” AIAA Paper 96-0884, January 1996.

<sup>21</sup>Vuillot, F., Dupays, J., Lupoglazoff, N., Basset, T., and Daniel, E., “2-D Navier-Stokes Stability Computations for Solid Rocket Motors: Rotational, Combustion and Two-Phase Flow Effects,” AIAA Paper 97-3326, July 1997.

<sup>22</sup>Lupoglazoff, N., and Vuillot, F., “Numerical Simulation of Vortex Shedding Phenomenon in Two-Dimensional Test Case Solid Rocket Motors,” AIAA Paper 92-0776, January 1992.

<sup>23</sup>Couton, D., Doan-Kim, S., and Vuillot, F., “Numerical Simulation of Vortex-Shedding Phenomenon in a Channel with Flow Induced through

Porous Wall,” *International Journal of Heat & Fluid Flow*, Vol. 18, No. 3, 1997, pp. 283-296.

<sup>24</sup>Couton, D., Doan-Kim, S., and Vuillot, F., “Numerical Simulation of Vortex-Shedding Phenomenon in a Channel with Flow Induced through Porous Wall,” *International Journal of Heat and Fluid Flow*, Vol. 18, No. 3, 1997, pp. 283-296.

<sup>25</sup>Ugurtas, B., Avalon, G., Lupoglazoff, N., and Vuillot, F., “Numerical Computations of Hydrodynamic Instabilities inside Channels with Wall Injection,” AIAA Paper 99-2505, June 1999.

<sup>26</sup>Prévost, M., Vuillot, F., and Traineau, J. C., “Vortex-Shedding Driven Oscillations in Subscale Motors for the Ariane 5 MPS Solid Rocket Motors,” AIAA Paper 96-3247, July 1996.

<sup>27</sup>Culick, F. E. C., “Stability of Longitudinal Oscillations with Pressure and Velocity Coupling in a Solid Propellant Rocket,” *Combustion Science and Technology*, Vol. 2, No. 4, 1970, pp. 179-201.

<sup>28</sup>Culick, F. E. C., “Acoustic Oscillations in Solid Propellant Rocket Chambers,” *Acta Astronautica*, Vol. 12, No. 2, 1966, pp. 113-126.

<sup>29</sup>Culick, F. E. C., “Rotational Axisymmetric Mean Flow and Damping of Acoustic Waves in a Solid Propellant Rocket,” *AIAA Journal*, Vol. 4, No. 8, 1966, pp. 1462-1464.

<sup>30</sup>Culick, F. E. C., “The Stability of One-Dimensional Motions in a Rocket Motor,” *Combustion Science and Technology*, Vol. 7, No. 4, 1973, pp. 165-175.

<sup>31</sup>Culick, F. E. C., “Stability of Three-Dimensional Motions in a Rocket Motor,” *Combustion Science and Technology*, Vol. 10, No. 3, 1974, pp. 109-124.

<sup>32</sup>Culick, F. E. C., “Rotational Axisymmetric Mean Flow and Damping of Acoustic Waves in a Solid Propellant Rocket,” *Journal of Propulsion and Power*, Vol. 5, No. 6, 1989, pp. 657-664.

<sup>33</sup>Culick, F. E. C., “Combustion Instabilities in Propulsion Systems,” *American Society of Mechanical Engineers, Noise Control and Acoustics Division*, Vol. 4, 1989, pp. 33-52.

<sup>34</sup>Culick, F. E. C., and Yang, V., “Prediction of the Stability of Unsteady Motions in Solid Propellant Rocket Motors,” *Nonsteady Burning and Combustion Stability of Solid Propellants*, Vol. 143, edited by L. De Luca, E. W. Price, and M. Summerfield, AIAA Progress in Astronautics and Aeronautics, Washington, DC, 1992, pp. 719-779.

- <sup>35</sup>Culick, F. E. C., "Combustion Instabilities in Propulsion Systems," *Unsteady Combustion*, Kluwer Academic Publishers, 1996, pp. 173-241.
- <sup>36</sup>Chibli, H. A., Majdalani, J., and Flandro, G. A., "Fundamental Growth Rate Corrections in Rocket Motor Stability Calculations," AIAA Paper 2002-3610, July 2002.
- <sup>37</sup>Flandro, G. A., and Majdalani, J., "Aeroacoustic Instability in Rockets," *AIAA Journal*, Vol. 41, No. 3, 2003, pp. 485-497.
- <sup>38</sup>Flandro, G. A., "Solid Propellant Acoustic Admittance Corrections," *Journal of Sound and Vibration*, Vol. 36, No. 3, 1974, pp. 297-312.
- <sup>39</sup>Flandro, G. A., "Approximate Analysis of Nonlinear Instability with Shock Waves," AIAA Paper 82-1220, July 1982.
- <sup>40</sup>Flandro, G. A., "Energy Balance Analysis of Nonlinear Combustion Instability," *Journal of Propulsion and Power*, Vol. 1, No. 3, 1985, pp. 210-221.
- <sup>41</sup>Flandro, G. A., "Effects of Vorticity on Rocket Combustion Stability," *Journal of Propulsion and Power*, Vol. 11, No. 4, 1995, pp. 607-625.
- <sup>42</sup>Terrill, R. M., "Laminar Flow in a Uniformly Porous Channel," *The Aeronautical Quarterly*, Vol. 15, 1964, pp. 299-310.
- <sup>43</sup>Flandro, G. A., "On Flow Turning," AIAA Paper 95-2530, July 1995.
- <sup>44</sup>Chibli, H. A., Majdalani, J., and Flandro, G. A., "Improved Energy Normalization Function in Rocket Motor Stability Calculations," AIAA Paper 2003-5113, July 2003.
- <sup>45</sup>Van Moorhem, W. K., "Flow Turning in Solid-Propellant Rocket Combustion Stability Analyses," *AIAA Journal*, Vol. 20, No. 10, 1982, pp. 1420-1425.
- <sup>46</sup>Lupoglazoff, N., and Vuillot, F., "Numerical Simulations of Parietal Vortex-Shedding Phenomenon in a Cold-Flow Set-Up," AIAA Paper 98-3220, July 1998.
- <sup>47</sup>Lupoglazoff, N., and Vuillot, F., "Parietal Vortex Shedding as a Cause of Instability for Long Solid Propellant Motors. Numerical Simulations and Comparisons with Firing Tests," AIAA Paper 96-0761, January 1996.